

Dynamical Aspects

Thus far, apart from occasional incursions into the realm of time-dependent phenomena, we have mainly been concerned with describing the geometric aspects of those fractal structures which are found in nature. These, however, have nearly always been the geometric aspects of a time-evolving system. Thus, we have successively examined ordinary and fractional Brownian motion (some of whose features are related to the present chapter), turbulent and chaotic phenomena, and the growth of aggregates whose dynamic scaling laws might also have been included in this chapter. Although these different aspects are interconnected, during this chapter, we shall devote ourselves to studying purely kinetic or dynamic characteristics.

5.1 Phonons and fractons

5.1.1 Spectral dimension

The question of spectral dimension is closely related to the problem of finding the density of vibration modes, or spectral density, in a fractal lattice. The spectral density is a very important quantity which is involved in problems concerning relaxation, transport, adsorption, etc.

Here we are interested in the component of the spectral density's behavior which is due to the lower frequencies. This corresponds to the long term behavior, that is, in the case of diffusion for example, to times that allow the explanation of the large scale structure of the system, which is sensitive to its fractal geometry, to be undertaken. In a d -dimensional Euclidean lattice this behavior is simple: the number of modes with frequency less than ω varies as ω^d :

$$N(\omega) \propto \omega^d \quad (5.1-1)$$

so, the spectral density, defined by $dN(\omega) = \rho(\omega) d\omega$ is such that

$$\rho(\omega) \propto \omega^{d-1}, \quad \omega \rightarrow 0. \quad (5.1-2)$$

Is there an equally simple expression for a fractal? Shender (1976) and Dhar (1977) proposed a power-law behavior for a self-similar fractal,

$$N(\omega) = \int_0^\omega \rho(\omega') d\omega' \quad \underset{\omega \rightarrow 0}{\propto} \quad \omega^{d_s}, \quad (5.1-3)$$

where d_s is called the *spectral dimension*.

Scaling law arguments have allowed Rammal and Toulouse (1983) to relate this exponent to the fractal dimension D and the scaling law satisfied by each separate mode.

Relation between the spectral and fractal dimensions

(i) Consider a fractal lattice composed of identical masses, linked by M identical elastic bonds in a cube of side L . Due to its fractal nature, change of scale by a factor b gives

$$M(bL) \propto b^D M(L),$$

so that the mode density (which depends on the number of elastic bonds) in a volume of side bL is

$$\rho_{bL}(\omega) \propto b^D \rho_L(\omega).$$

(ii) As the modes are discrete and ω is positive (there is a ground state), let us make a bijection between modes. Then, *if there is a b* such that

$$\omega(bL) \propto b^{-\zeta} \omega(L),$$

we can deduce that

$$\rho_{bL}(\omega) \propto b^\zeta \rho_L(b^\zeta \omega).$$

(We shall verify this hypothesis in the case of Sierpinski's gasket.)

From the two relations between ρ_{bL} and ρ_L , we have:

$$\rho_L(\omega) \propto b^{-D+\zeta} \rho_L(b^\zeta \omega).$$

So for power-law behavior in ρ , it is sufficient to choose b such that $b^\zeta \omega = \text{const.}$:

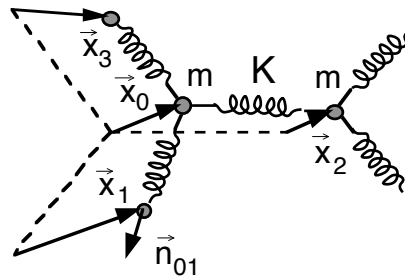
$$\rho_L(\omega) \propto \omega^{d_s-1} \quad \text{with} \quad d_s = D/\zeta. \quad (5.1-4)$$

But what was the point of establishing this relation when we do not know ζ ? In fact, as an example will show, ζ can be calculated — sometimes exactly, more often approximately — by a method of renormalization. This method is a practical illustration of the so-called renormalization group transformations (in this case in real space).

Example of calculation of the excitation spectrum by renormalization: the Sierpinski's gasket

Consider the gasket of side L, below, in which the vertices of the triangles of mass m are linked by springs of tension K. The coordinates $x_1, x_2, x_3, y_1, y_2, y_3, X_1, X_2, X_3$, etc., represent small displacements of the masses m about their equilibrium position. These displacements are vectors which may be restricted to the plane of the lattice if planar modes alone are being considered. The equations of motion are of the form

$$m \frac{d^2 \vec{x}_0}{dt^2} = \vec{F}_{01} + \vec{F}_{02} + \vec{F}_{03} \quad \text{with} \quad \vec{F}_{0i} = K (\vec{x}_i - \vec{x}_0) \cdot \vec{n}_{0i} \quad \vec{n}_{0i} \quad .$$



Such a system of equations is, however, too difficult to solve. To simplify it we carry out a *purely scalar calculation*, that is, using a single component per site. This is not a very realistic approximation for a network of springs (or a lattice of atoms, etc.), but gives us a first idea of the dynamic behavior of a fractal system. It may, however, be interpreted as a model of

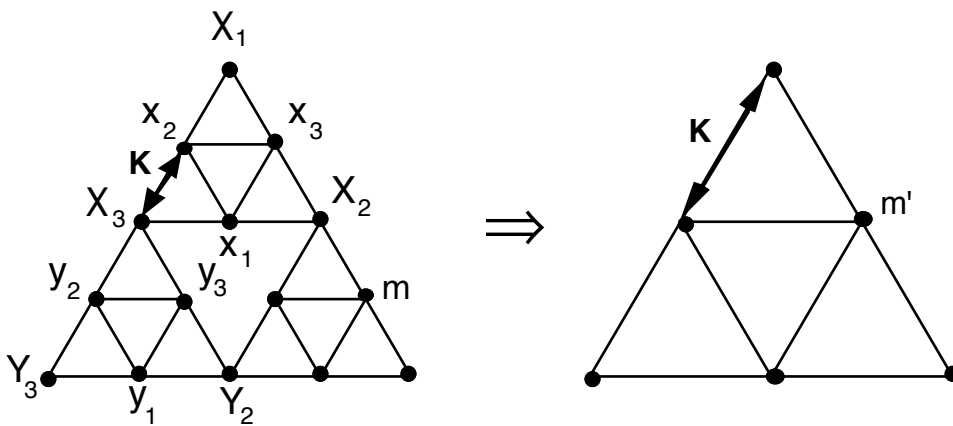


Fig. 5.1.1. Renormalization of a Sierpinski gasket: the renormalization consists in finding an iteration n such that when it is applied to iteration n - 1 of the hierarchy, a system having the same physical characteristics is obtained. If the tension K in the springs is left unchanged, we must alter (renormalize) the masses ($m \rightarrow m'$) (see the text).

entropic vibration,¹ the component x_i corresponding to a local entropy. Sierpinski's gasket then leads to a system of coupled, linear equations which can be solved by renormalization. Moreover, thanks to its linearity the system may be studied at a fixed frequency, ω .

The $x, y\dots$ denote the "displacements" of the vertices of the smallest triangles (of side l); $X, Y\dots$ the displacements of the vertices of the triangles of side $l' = 2l$, etc.

The equations of motion are

$$\begin{aligned} m\omega^2 x_1 &= K\{(x_1 - x_2) + (x_1 - x_3) + (x_1 - X_3) + (x_1 - X_2)\}, \\ m\omega^2 x_2 &= K\{4x_2 - x_1 - x_3 - X_1 - X_3\}, \\ m\omega^2 x_3 &= K\{4x_3 - x_1 - x_2 - X_1 - X_2\}. \end{aligned} \quad (5.1-5)$$

On eliminating x_3 , these three equations give

$$x_1 = f_1(X_1, X_2, X_3), \quad x_2 = f_2(X_1, X_2, X_3).$$

The same calculation is carried out for y_2, y_3 and the results brought together as

$$m\omega^2 X_3 = K [4X_3 - x_1 - x_2 - y_2 - y_3].$$

We thus find an equation similar to Eq. (5.1-5) for X_3 as a function of $(X_1, X_2; Y_2, Y_3)$, but where the mass has been "renormalized":

$$m' = m [5 - m\omega^2/K]. \quad (5.1-6)$$

The dimensionless parameters of the problem are $\alpha = m\omega^2/K$ and $\alpha' = m'\omega^2/K = m\omega'^2/K$ (the latter equality is obtained by conserving the mass while changing the frequency), α and α' being related by the recurrence relation

$$\alpha' = \alpha(5 - \alpha). \quad (5.1-7)$$

Now, instead of renormalizing the mass ($m \rightarrow m'$), we renormalize the frequencies ($\omega \rightarrow \omega'$) leaving the mass unchanged: in other words, the gasket remains unchanged on renormalization. For a change of scaling $b = 1/2$ ($L = 4l \rightarrow L = 2l'$) the square of the frequency is multiplied by 5 if, in (5.1-7), we neglect the term in α^2 in the neighborhood of $\omega = 0$. This gives the relation

$$(\omega_{L/2})^2 = 5 (\omega_L)^2 \quad \text{of the form} \quad \omega_{bL} = b^{-\zeta} \omega_L.$$

From this we can find ζ , then, using the relation (5.1-4) obtained for d_s ,

$$\zeta = \frac{1}{2} \frac{\ln 5}{\ln 2} \quad \text{and} \quad d_s = \frac{D}{\zeta} = 2 \frac{\ln 3}{\ln 5} \cong 1.364. \quad (5.1-8)$$

We have thus found the exponent d_s of the density of "scalar vibration" states of the Sierpinski gasket.

¹ The elasticity of the material then being, as with rubber for instance, of entropic origin.

The various dimensional exponents satisfy the inequalities $d_s \leq D < d$. We shall return to the general case, where the displacements of the masses are represented by vectors, when we come to look at the elastic properties of disordered systems displaying a percolation structure. For the moment, this calculation of the spectral dimension will suffice for our needs.

Note however that it is possible to construct fractals of finite ramification, generalizing the Sierpinski gasket, and for which the value of d_s may be calculated exactly. Hilfer and Blumen (*Fractals in Physics*, 1986, p. 33) have shown that the possible values of d_s are dense in the interval $[1,2]$ for a suitable choice of two-dimensional fractal lattice. Furthermore, by enlarging the space by direct multiplication, structures can be constructed for which d_s is dense in the interval $[1,\infty]$.

Dispersion relations

This term denotes the relation between the wavelength of a vibration mode and its frequency. For normal elastic lattices this relation is linear: waves of wavelength Λ propagate at the speed of sound v , and the dispersion relation can be written simply as

$$\omega \propto v/\Lambda \quad . \quad (5.1-9a)$$

To find the dispersion relation for the modes of vibration in fractal structures, let us consider a mode of “wavelength” Λ according to the d spatial directions. In fact we should not really talk about wavelength in this situation but instead about localization length, as sinusoidal waves do not propagate in such media. This mode defines vibration modes covering spatial domains V_Λ , of spatial extent Λ^d , and a number Λ^D of elastic bonds in the fractal lattice. It also has frequency ω . All other modes of lower frequency correspond to larger dimensions than Λ and for these modes the bonds in V_Λ may be taken as vibrating in phase. Those modes of higher frequency than ω and of lower wavelength than Λ , are invariant under changes in the boundary conditions of the domain V_Λ , so that the integrated spectrum of the low-frequency modes, absent from the localization domain V_Λ ,

$$\Lambda^D \int_0^\omega \omega^{d_s - 1} d\omega$$

is independent of Λ and ω , because of the scale invariance of the fractal structure (see, e.g., Alexander, 1989). Hence, the *anomalous dispersion relation* for modes of vibration in fractal structures is,

$$\omega \propto \Lambda^{-D/d_s} \quad . \quad (5.1-9b)$$

Localized modes of vibration associated with fractal structures are known as *fractons*. Experimental confirmation of the existence of fractons will be given in Sec. 5.1.4.

Lévy and Souillard (1987) have proposed that the form of the wave function of a fracton (i.e., the *mean* spatial distribution of its amplitude of vibration) be given by

$$\phi(\omega) \propto \frac{\Lambda^{D/2}}{r^{d-D}} \exp\left\{-\frac{1}{2}\left(\frac{r}{\Lambda}\right)^{d_\phi}\right\} \quad \text{where } 1 < d_\phi < d_{\min}. \quad (5.1-10)$$

(d_{\min} is the chemical dimension or the dimension of connectivity, see Sec. 1.5.1). This function decreases rapidly with the distance r and has a range of the order of Λ .

In a recent study, Bunde et al. have suggested that fractons have a very multifractal character, and that the vibrational amplitudes at a given frequency and fixed distance from the center of mass of a *typical* fracton, may be characterized, as a function of the amplitude, by a logarithmic size distribution. It would then no longer be possible to define the localization length describing the exponential decrease of these amplitudes uniquely.

5.1.2 Diffusion and random walks

Let us now consider the problem of a particle diffusing through a fractal lattice. Let $P_i(t)$ be the probability of finding the particle at vertex i in a fractal lattice at time t . Let W_{ij} be the probability per unit time of a particle at site j jumping to site i . Balancing these probabilities gives the time evolution equation

$$\frac{dP_i(t)}{dt} = - \sum_j W_{ij} \{P_i(t) - P_j(t)\}. \quad (5.1-11)$$

To solve a set of coupled equations of this kind, we seek an expression for the probability $P(i,t | k,0)$ of finding the particle at site i at time t , given that it was at site k at time 0, by expanding it in terms of the eigenstates $\psi_i^{(\alpha)}$ of the system in the form,

$$P(i,t | k,0) = \text{Re} \sum_\alpha \psi_i^{(\alpha)*} \psi_k^{(\alpha)} e^{-z_\alpha t} \quad \text{with the initial condition } P(i,0 | k,0) = \delta_{ik}.$$

The eigenvalues of the evolution equation are such that

$$\sum_j T_{ij} \psi_j^{(\alpha)} = \lambda_\alpha \psi_i^{(\alpha)}, \quad \text{where } T_{ij} = W_{ij} - \delta_{ij} \sum_h W_{ih}.$$

Comparing this with the evolution equation we find that $\lambda_\alpha \equiv -z_\alpha$ for diffusion, while $\lambda_\alpha \equiv -(\omega_\alpha)^2$ for the equivalent vibration problem, because of the second time derivative.

Knowing the P_i allows all the quantities describing the transport of this particle to be calculated. The mean square distance covered is then given by (the P_i being normalized: $\sum P_i = 1$)

$$\langle R^2(t) \rangle = \sum_i R_i^2 P_i(t). \quad (5.1-12)$$

Here again, since the lattice is self-similar, we may expect power-law behavior as a function of time. So, let us write

$$\langle R^2(t) \rangle \propto t^{2/d_w} \tag{5.1-13}$$

where d_w is the fractal dimension of the walk with t taken as a measure (of the “mass”). d_w is as important an exponent as the fractal and spectral dimensions to which it is related. Let us suppose for simplicity that the W_{ij} are equal to W for the jumps between first neighbors, and zero otherwise. In a Euclidean lattice this leads simply to a Brownian walk whose behavior has already been shown to be:

$$\langle R^2(t) \rangle \propto t \tag{5.1-14}$$

The path of the Brownian motion, t steps within a radius R , has a fractal dimension (refer to Sec. 2.2.1)

$$d_w = 2 \tag{5.1-15}$$

The situation for a fractal lattice is not the same; it is harder for the particle to diffuse and so we expect that $d_w > 2$.

Let us now take the Fourier transform of the evolution equation. Defining

$$\tilde{P}_i(z) = \int_0^\infty e^{-zt} P_i(t) dt \tag{5.1-16}$$

where e is the Fourier transform of $P_i(t)$ and f is the Fourier transform of $P_i(z)$.

$$-z \tilde{P}_i = \sum_{j=i+\delta} W (\tilde{P}_j - \tilde{P}_i), \tag{5.1-17}$$

$j = i + \delta$ denoting the first neighbors of i . We see that this equation is the same as Eq. (5.1-5), if the transformation $\omega^2 \leftrightarrow z$, concerning the (scalar) harmonic vibrations of the lattice is made. Hence, we may use all the arguments of the previous subsection.

Denote by $\rho_D(z)$ the density of modes (i.e., of the eigenvalues) of the diffusion equation. From above,

$$\int_0^z \rho_D(\omega') d\omega' \underset{z \rightarrow 0}{\propto} z^{d_s/2} \tag{5.1-18}$$

In particular, this allows us to determine the probability that the random walk will return to the origin after a time t ,

$$P_{\text{return}}(t) = \int_0^\infty \rho_D(z) e^{-zt} dz \propto t^{-d_s/2} \tag{5.1-19}$$

To prove this relation, we take the probability of a return to the origin to be inversely proportional to the number of visited sites or equivalently to the mean probability of occupying a site, hence

$$P_{\text{return}}(t) = \langle P_i(t) \rangle = \frac{1}{N} \sum_{i=1}^N P_i(t) = \frac{1}{N} \sum_{\alpha=1}^N \exp(-z_{\alpha} t)$$

so, finally

$$P_{\text{return}}(t) = \int_0^{\infty} \rho_D(z) e^{-zt} dz.$$

We can use a scaling argument to determine the form (at large t) of $P(\vec{r}, t)$. There is, in fact, a unique scaling length involved in this problem, namely the diffusion length

$$\lambda(t)^2 = \langle R^2(t) \rangle, \quad \text{hence we may write}$$

$$P(\vec{r}, t) \propto \lambda^{-D} f\left(\frac{\vec{r}}{\lambda}\right), \quad (5.1-20)$$

where the coefficient λ^{-D} is imposed by the normalization of $P(\vec{r}, t)$ over the fractal domain.

Therefore, $P(0, t) \propto \lambda^{-D}$, hence

$$\lambda \propto t^{d_s/2D}$$

and, since $\lambda \propto t^{1/d_w}$, we have: $P(\vec{r}, t) \propto t^{-d_s/2} f\left(\frac{\vec{r}}{t^{1/d_w}}\right)$,

and

$$\boxed{d_w = \frac{2D}{d_s}}. \quad (5.1-21)$$

In particular, we have $d_w = 2$ when $D = d_s (= d)$.

In very general terms, the diffusion profile, that is, the probability density of random walkers in random systems, has a stretched exponential structure. i.e., the function f above has the form

$$f(x) \propto \exp(-x^u), \quad \text{where } u = d_w/(d_w - 1).$$

(See, e.g., Havlin and Bunde, 1989, on this point.)

Furthermore, the anomalous transport of particles in disordered structures is sensitive to additional disorder due, for instance, to a nonuniform probability distribution for particles jumping from one site to another, or even to the existence of a bias (systematic external force acting on the particles) (Bunde in Stanley and Ostrowsky, 1988).

Link with modes of vibration in fractal structures

We have just established a relation relating the scaling lengths λ (mean distance covered) of physical phenomenon to their time scales via the density of states. This relation also applies to (scalar) vibrational systems, as the structure of the equations remains unchanged under the transformation $\omega^2 \leftrightarrow z$. This means that the characteristic length Λ of a fracton and its frequency (reciprocal of a time) are related by the relation

$$\Lambda \propto (\omega^2)^{-d_s/2D}.$$

The anomalous dispersion relation of the vibrational modes of elastic fractal structures is thus, as we described above [Eq. (5.1-9)],

$$\omega \propto \Lambda^{-D/d_s}.$$

5.1.3 Distinct sites visited by diffusion

First, the following remark needs to be made: the spectral dimension d_s characterizes the *mean* number $S(N)$ of *distinct* sites visited after N steps.

For Euclidean lattices this relation is exact:

$$S(N) \propto \begin{cases} N^{1/2} & \text{when } d = 1 \\ N/\ln N & \text{when } d = 2 \\ N & \text{when } d \geq 3, \end{cases} \left. \vphantom{\begin{cases} N^{1/2} \\ N/\ln N \\ N \end{cases}} \right\} \text{the walk is recurrent.}$$

there is a nonzero chance to escape to infinity.

For a fractal lattice, the number of distinct sites visited is proportional to R^D , where R is the mean radius of the walk, hence *via* Eqs. (5.1-13) and (5.1-21),

$$S(N) \propto N^{d_s/2} \quad \text{if } d_s \leq 2, \quad (5.1-22)$$

and obviously no more than N sites may be visited after N steps,

$$S(N) \propto N \quad \text{if } d_s > 2. \quad (5.1-23)$$

From this we conclude that $d_s = 2$ is a *critical spectral dimension*² for random walks, that is to say

- (i) if $d_s \leq 2$ the walk is recurrent and the exploration is called *compact*;
- (ii) if $d_s > 2$ the walk is transitory and the majority of sites will never be visited, so the exploration is *noncompact*.

Considerations about the number of distinct sites visited during a diffusion process are important for many physical phenomena. An example of this is provided by diffusion in a trap possessing medium.

Diffusion in the presence of traps

Consider particles (or excitations), diffusing in a medium until they meet a trap which either annihilates or stops them for a very long time. How does the particle or excitation density evolve with time when this medium is a fractal structure? This is an important feature in numerous problems of charge transport, mainly in semiconductors (disordered alloys).

The time evolution can be described by calculating the *probability of survival* $\phi(N)$ of a particle after N steps,

$$\phi(N) = \langle (1 - x)^{R(N)} \rangle,$$

²Not to be confused with the dimension of the walk itself!

where $R(N)$ is the number of distinct sites visited and x is the density of traps; its mean, whose behavior we have just examined, is given exactly by $S(N) = \langle R(N) \rangle$.

At relatively short time scales,

$$\phi(N) \propto \exp [- xS(N)], \quad (5.1-24)$$

a behavior which has been verified experimentally to a high degree of precision.

At relatively long time scales, $\phi(N)$ can be shown to behave theoretically like a “stretched” exponential, that is, as

$$\phi(N) \propto \exp \left(- c \{ xS(N) \}^{2/(d_s + 2)} \right). \quad (5.1-25)$$

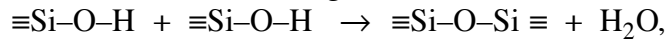
This may be explained by the presence of large regions without traps which are rarer the larger they are. In practice, except when $d = 1$, this behavior is very difficult to observe experimentally. Note that the problem of diffusion with traps, in a homogeneous medium, can be solved exactly and that the above results are in good agreement with the homogeneous case if d_s is simply changed to d (Havlin in Avnir, 1989).

5.1.4 Phonons and fractons in real systems

Localized vibration modes can be observed in real systems. Investigation by means of light and neutron scattering has demonstrated the existence of fractons and their essential properties.

The clearest experiments have been carried out on silica aerogels, but other experiments have used epoxy resins, solid electrolytic glasses of silver borate, and hydrogenized amorphous silicon. The experiments are tricky and the results not always convincing, so it is indispensable to have a wide range of evidence from different techniques. The case of aerogels, for which there are numerous measurements, covering a wide range of techniques, is discussed in detail. Polymers and gels are introduced in Sec. 3.5.1.

We have already had occasion to talk about silica gels when we were describing the measurement of the fractal dimension of aggregates (small angle scattering in Sec. 3.4.2). In very schematic terms, aerogels are prepared in the following manner: compounds $\text{Si}(\text{OR})_4$ are hydrolyzed in the presence of alcohol diluting the product to form groups $\equiv\text{Si}-\text{O}-\text{H}$. These groups “polycondense” to form siloxane bridges,



thereby producing a solid lattice based on SiO_4 tetrahedra. Aggregates grow around the nucleation sites until they stick to each other, leading to the construction of percolation clusters (cf. Fig. 3.5.3). Thus, a gel is formed. With this method of production the final product is called an alcogel as the solvent is

made up of alcohols R–OH issuing from the initial product. The alcogel is then dried³ to remove the interstitial fluid, yielding an *aerogel*.

To simplify matters, let us suppose that up to a distance ξ the final gel is a fractal of dimension D , and that it is homogeneous at longer distances. This is tantamount to bonds continuing to form between the aggregates after the gelation point has been passed. Knowing D and the density $\rho = \rho(\xi)$ of the material, ξ may be found:

$$\rho(\xi)/\rho(a) = (\xi/a)^{D-d} \quad (d = 3),$$

where a is the size of the grains (the compact aggregates at the basis of the fractal structure) and $\rho(a) \cong 2,000 \text{ kg/m}^3$, close to the density of pure silica.

The phonon–fracton transition

At distances large compared with ξ , in other words, for low-frequency vibrations, the fractal behavior plays no part as the fractal domains vibrate as one. The gels then behave like a normal solid elastic of dimension L , in which phonons are propagated at the speed of sound⁴ v , with the dispersion relation $\omega \propto v/\lambda$, and density of states $\rho_L(\omega) \propto L^d \omega^{d-1} = L^3 \omega^2$.

At short distances, the fractal nature should bring about the existence of localized fractons, with the dispersion law $\omega \propto \lambda^{-D/d_s}$ and density of states $\rho_L(\omega) \propto L^D \omega^{d_s-1}$.

The fracton and phonon régimes meet when λ is of the order of ξ . This defines a crossover frequency $\omega_{cr} = (\omega_{cr}/2\pi)$ which depends on the mean density ρ . Thus,

$$\omega_{cr} \propto \rho^{D/d_s(3-D)}. \quad (5.1-26)$$

As mentioned above, the experimental observation of fractons is tricky (see, e.g., Courtens et al. in Pietronero, 1989, p. 285).

Light scattering experiments (Brillouin scattering, Raman scattering) have enabled Pelous and his collaborators at Montpellier and Courtens at IBM-Zurich to display the existence of fractons and to determine their essential characteristics. Courtens et al. (1988) have estimated the fractal and spectral dimensions to be $D \cong 2.4$ and $d_s \cong 1.3$, respectively. Furthermore, they have found the crossover frequency to be $\omega_{cr} \propto \rho^{2.97}$. Vacher et al. (1990) have measured the density of vibrational states in silica aerogels by a combination of inelastic, incoherent neutron spectroscopy and Brillouin scattering measurements. These measurements clearly demonstrate an extended fracton regime.

³ A hypercritical drying process is used to avoid liquid–vapor interface tensions which tend to cause the deterioration of the fragile structure of the skeleton of siloxanes.

⁴ Here, only consider acoustic phonons, propagating by compression, are considered.

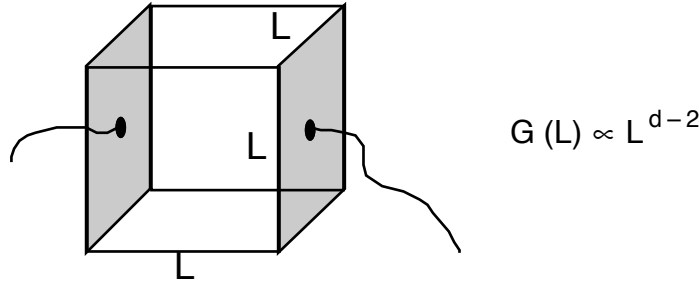
Several authors have also tried to exhibit fracton-type behavior in amorphous materials (such as hydrogenized amorphous silicon), in certain epoxy resins, in ionic superconducting silver borate glasses, and at the interfaces of sodium colloids in NaCl. In the diluted antiferromagnetic composite $Mn_{0.5}Zn_{0.5}Fe_2$, Birgeneau and Uemura (1987) observed a crossover from a magnon régime change to a fracton régime (characterized by a very wide band).

For the correct interpretation of experiments on propagation and localization in these materials, a thorough understanding of their structure is important; this, however, is far from being the case. The structure of aerogels, for example, is still subject to debate: a percolation-type structure of elementary entities (SiO_4 or mini-aggregates), an aggregation-type structure and a hierarchical sponge-like structure have all been proposed (Maynard, 1989). Similarly, fracton modes are not clearly understood. Certain measurements suggest an interpretation using the scalar fracton model (these we calculated in Sec. 5.1.1 on a Sierpinski gasket), others seem rather to correspond to vectorial fractons. Several fracton branches (corresponding to compression and flexion modes) were observed by Vacher et al. (1990), who used a combination of Raman and neutron spectroscopy to display a succession of régimes in the vibrational dynamics of two aerogels with different microstructures. In this way, three crossovers were observed: at low frequencies, the change from a phonon to a fracton régime; at high frequencies, the change from fracton to particle modes (Porod régime in Q^{-4}); while at intermediate frequencies, there is a crossover, attributed by the authors, to the change from compression to flexion modes. The values obtained for the spectral dimension (and for the fractal dimension) depend on the microstructure. They found $D \cong 2.4$, $d_s(\text{flexion}) \cong 1.3$, and $d_s(\text{compression}) \cong 2.2$ in one case, and $D \cong 2.2$, $d_s(\text{flexion}) \leq 1$, and $d_s(\text{compression}) \cong 1.7$ in the other. These values suggest that internal connections occur more frequently here than in a three-dimensional percolation lattice (the tensorial elasticity of a percolation lattice is treated in Webman and Grest, 1985). Sec. 5.2.4, on the viscoelastic transition, may also be consulted on this subject.

5.2 Transport and dielectric properties

5.2.1 Conduction through a fractal

For an (ordinary) Euclidean object the conductance is given by a simple power of its transverse dimensions. For a uniform conductor in the shape of a cube of side L with two opposite faces conducting, the conductance $G(L)$ of this object varies as L^{d-2} .



In addition, the conductivity, Σ ,⁶ and the diffusion coefficient, \mathcal{D} , are related by the Nernst–Einstein equation

$$\Sigma = \frac{ne^2}{kT} \mathcal{D} \quad (5.2-1)$$

(n is the concentration of charges e) and the diffusion coefficient can be calculated from $\langle r^2 \rangle = 2 \mathcal{D} t$.

For a fractal, the Nernst–Einstein equation still holds for an effective coefficient of diffusion $\mathcal{D}_{\text{eff}}(r)$, defined by

$$\mathcal{D}_{\text{eff}}(r) = \frac{1}{2} \frac{d\langle r^2 \rangle}{dt} \quad (5.2-2)$$

from Sec. 5.1.2:

$$\mathcal{D}_{\text{eff}}(r) \propto t^{d_s/D-1}, \quad (5.2-3)$$

that is, in terms of the mean distance $r = \sqrt{\langle r^2 \rangle} \propto t^{d_s/2D}$:

$$\mathcal{D}_{\text{eff}}(r) = r^{-\theta} \quad \text{with} \quad \theta = 2 \left(\frac{D}{d_s} - 1 \right) \quad (5.2-4)$$

The conductance may also be determined:

$$G(r) \propto \sigma(r) r^{D-2} \propto r^{D(1-2/d_s)}. \quad (5.2-5)$$

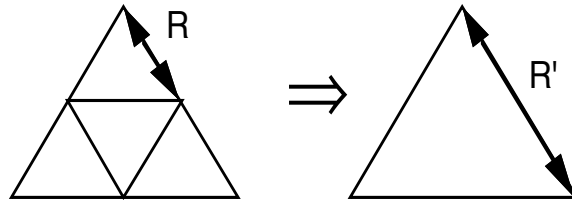
Thus, conductance for a fractal structure depends anomalously on the dimension of the sample via a power law:

$$G(r) \propto r^{-\tilde{\zeta}} \quad \text{where} \quad \tilde{\zeta} = \frac{D}{d_s} (2 - d_s). \quad (5.2-6)$$

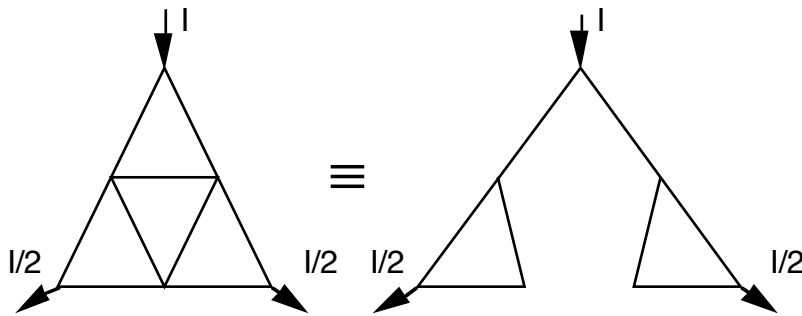
It is interesting to compare this behavior with the results of Sec. 5.1.2. If $d_s < 2$ the walk is recurrent (the same points are passed indefinitely) and in this case the conductance decreases with the distance r : a localization phenomenon is produced. In particular, vibrations do not propagate when $d_s < 2$, but instead remain localized within certain regions of the fractal structure.

⁶ The conductivity Σ relates the current density to the electric field $\mathbf{i} = \Sigma \mathbf{E}$, while the conductance G relates the current to the applied potential through $I = G(L) V$.

By way of an example, let us calculate explicitly the conductance of a Sierpinski gasket. As in the case of vibrations, renormalization is used for these calculations. Each set of three triangles (with a corner pointing upwards), whose sides have resistance R , is replaced by a single triangle with sides of resistance R' :



The resistance can be calculated exactly by taking the symmetry into account, and by noticing that the following two networks, with a current I flowing through them are electrically equivalent,



hence $R' = 5/3 R$. Therefore, at the n th iteration the conductance (which is in $1/R$) is given by

$$\left\{ \begin{array}{l} G^{(n)} = \left(\frac{3}{5}\right)^n G_0 \\ L^{(n)} = 2^n \end{array} \right. \quad \text{thus} \quad \frac{\ln G}{\ln L} \Big|_{n \rightarrow \infty} = \frac{\ln (3/5)}{\ln 2} = D \left(1 - \frac{2}{d_s}\right)$$

giving $d_s = 2 (\ln 3/\ln 5)$. The result obtained for the Sierpinski gasket in Sec. 5.1.1 by numbering the vibration modes, is retrieved.

Comparison of the different approaches

It is instructive to compare approaches which deal with vibration in a fractal lattice with those dealing with diffusion or conduction in the same lattice. In the scalar case, the elastic energy can be written as

$$\frac{1}{2} \sum_{i,j} K_{ij} (x_i - x_j)^2,$$

where K_{ij} is the elastic constant between i and j . (All the K_{ij} with i and j nearest neighbors were taken equal to K in the example in Sec. 5.1.1.) Equilibrium for

these forces is found by minimizing this energy, or alternatively by putting $\omega = 0$ in the equations of motion [Eq. (5.1-5)]. Thus,

$$\sum_j K_{ij}(x_i - x_j) = 0. \quad (5.2-7)$$

If x_i is replaced by the potential v_i at site i and K_{ij} by the conductance Y_{ij} of the bond ij , this equation is identical to the Kirchoff equation for the same network.

Therefore, *the elastic constant of a network of springs behaves in the same way as the conductivity of an identical resistor network.*

5.2.2 Conduction in disordered media

One problem commonly found when dealing with disordered materials is that of determining the conductivity of a random mixture of two components of widely differing conductivities σ_1 and σ_2 ($\sigma_2 \gg \sigma_1$). An excellent review of this is in Clerc et al. (1990).

The conductivity depends on the relative concentrations of the two materials. Not surprisingly, the conductivity changes rapidly at the percolation threshold where a crossover takes place.

To help understand this phenomenon the following limiting cases may be considered:

- (i) metal-insulator transition, corresponding to $\sigma_1 = 0$, σ_2 finite;
- (ii) metal-superconductor transition, corresponding to σ_1 finite, σ_2 infinite.

In the first case, the conductivity varies just as it did for percolation (Fig. 3.1.2). Let p denote the concentration of the more highly conducting material (of conductivity σ_2). The material is an insulator when $p < p_c$; above p_c , the conductivity increases, and close to p_c it may be written (at least in a large network, neglecting the effects of finite size) as

$$\Sigma = 0, \quad p < p_c; \quad \Sigma \approx \sigma_2 (p - p_c)^\mu, \quad p \geq p_c \quad (5.2-8)$$

For percolation, the exponent μ (some authors use the notation t) is about 1.3 in two dimensions (see the table of dynamic exponents below).

In the second case, the conductivity of the material is finite when $p < p_c$; above the threshold, when percolation takes place, a superconducting path appears and the conductivity becomes infinite. Thus, we have

$$\Sigma \approx \sigma_1 (p_c - p)^{-s}, \quad p < p_c; \quad \Sigma = \infty, \quad p \geq p_c. \quad (5.2-9)$$

μ and s are critical transport exponents.

A network involving a metal-insulator transition is known as a *Random Resistor Network* (RRN). The corresponding diffusion problem has been around for a long time (de Gennes, 1976). A particle is constrained to diffuse through a percolation cluster. This situation is usually called the problem of the *ant in a labyrinth*.

A network involving a metal–superconductor transition is known as a *Random Superconductor Network* (RSN). The corresponding diffusion problem, in which a particle diffuses normally from one cluster to another, then infinitely quickly through each cluster, is usually (with a physicist’s humor) referred to as the problem of the *termite in a disordered network*.

General case

From these limiting cases and the assumption that scaling laws exist, the general behavior for a mixture of two finite conductivities σ_1 and σ_2 can be deduced (Straley, 1976). The two cases link up in the neighborhood of p_c where the critical behavior occurs.

A reasonable hypothesis now is to take Σ as dependent essentially on the ratio σ_1/σ_2 and on $p - p_c$:

$$\Sigma(p, \sigma_1, \sigma_2) \approx \sigma_1 f\left(\frac{\sigma_1}{\sigma_2}, p - p_c\right). \quad (5.2-10)$$

Then we assume the existence of a scaling law, that is, a dimensionless quantity⁷ dependent on σ_1/σ_2 and $p - p_c$. Suppose that dividing the ratio σ_1/σ_2 by a factor b , corresponds to a dilatation of $(p - p_c)$ by a factor b^λ . Then $(\sigma_2/\sigma_1)^\lambda (p - p_c)$ is a dimensionless quantity and the conductivity Σ has the general form

$$\Sigma \approx \sigma \left(\frac{\sigma_2}{\sigma_1}\right)^u g\left((p - p_c) \left(\frac{\sigma_2}{\sigma_1}\right)^\lambda\right). \quad (5.2-11)$$

The prefactor with exponent u gives the scaling behavior at $p = p_c$; λ and u remain to be determined.

Finally, we take Σ to be nonsingular for $p = p_c$ and adjust the general behavior to agree with the limiting behavior. Good limiting laws therefore require that when

$$v > 0, \quad g(v) \propto v^\mu$$

and that when

$$v < 0, \quad g(v) \propto v^{-s}$$

so that:

(i) when $p > p_c$ and $v \gg 0$,

$$\Sigma \approx \sigma_1 \left(\frac{\sigma_2}{\sigma_1}\right)^{u + \lambda \mu} (p - p_c)^\mu \approx \sigma_2 (p - p_c)^\mu$$

must be independent of σ_1 , hence

$$\lambda = \frac{1 - u}{\mu};$$

⁷ That is, in this case dilation invariant.

(ii) when $p < p_c$ and $v \ll 0$,

$$\Sigma \approx \sigma_1 \left(\frac{\sigma_2}{\sigma_1} \right)^{u - \lambda s} (p - p_c)^{-s} \approx \sigma_1 (p - p_c)^{-s}$$

must be independent of σ_1 , hence

$$\lambda = \frac{u}{s} .$$

Finally, we have (see Fig. 5.2.1)

$$\Sigma \approx \sigma_1 \left(\frac{\sigma_2}{\sigma_1} \right)^{\frac{-s}{s+\mu}} g \left((p - p_c) \left(\frac{\sigma_2}{\sigma_1} \right)^{\frac{1}{s+\mu}} \right) \quad (5.2-12)$$

This expression is very interesting as it allows us to generalize the case where the component resistances (bonds of the disordered network) are replaced, using analytic continuation, by complex impedances.

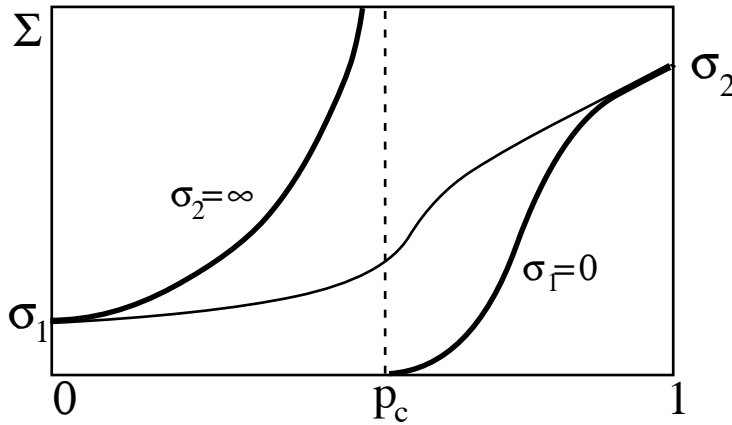


Fig. 5.2.1. Diagram showing the variation of conductivity as a function of the concentration p of the more conducting bonds in the network ($\sigma_2 \gg \sigma_1$). The curve $\sigma_1 = 0$ corresponds to the insulator–metal transition, the curve $\sigma_2 = \infty$ to the metal–superconductor transition. The intermediate curve represents the general case where both conductivities take finite values.

Particular case: at the percolation threshold $p = p_c$,

$$\Sigma \approx (\sigma_1)^{\frac{\mu}{s+\mu}} (\sigma_2)^{\frac{s}{s+\mu}} . \quad (5.2-13)$$

Thus, in two dimensions the duality between the networks (Bergmann, in Deutscher et al., 1983, Chap. 13; see also Clerc et al., 1990) gives $s = \mu$ and an exact result:

$$\Sigma(p = p_c) = \sqrt{\sigma_1 \sigma_2} . \quad (5.2-14)$$

Relation between μ and the spectral dimension d_s

Consider a random walk over the infinite percolation cluster when $p > p_c$. Two régimes are then observed: at short distances the medium appears to be a fractal of dimension D and this remains so up to a distance equal (on average) to the correlation length ξ . The correlation function is approximately of the form

$$g(r) \cong \frac{1}{r^{d-D}} \exp\left(-\frac{r}{\xi}\right). \quad (5.2-15)$$

Thus, when $\langle R^2(t) \rangle < \xi^2$ (that is, $t < t_\xi$), $\langle R^2(t) \rangle \propto t^{d_s/D}$.

On the other hand, for long times, when the diffusion distance $\sqrt{\langle R^2 \rangle}$ is greater than ξ , the medium appears homogeneous. Then the diffusion coefficient \mathcal{D} , which is time-independent, depends on $(p - p_c)$ as a power law whose exponent ρ ,

$$\langle R^2(t) \rangle \propto t \mathcal{D}(p) \propto t (p - p_c)^\rho \quad (5.2-16)$$

will be determined by linking up these two régimes:

$$\left\{ \begin{array}{l} \xi^2 \propto (t_\xi)^{d_s/D} \propto t_\xi \cdot (p - p_c)^\rho \\ \text{with } \xi^{-2} \propto (p - p_c)^{-2\nu} \end{array} \right.$$

Identifying these two behaviors in the neighborhood of p_c and expressing t_ξ as a function of $(p - p_c)$ gives

$$\frac{d_s}{D} = \frac{2\nu}{2\nu + \rho}. \quad (5.2-17)$$

Now, we introduce the Nernst–Einstein relation $\Sigma(p) \propto \mathcal{D}_0(p)$, where $\mathcal{D}_0(p)$ corresponds to the diffusibility averaged over all sites. As only those particles placed in the infinite cluster contribute to $\langle R^2 \rangle$ as $t \rightarrow \infty$, the diffusion coefficient must be normalized relative to the probability $P(p)$ that the departure point belongs to the infinite cluster. Thus,

$$\mathcal{D}(p) = \frac{\mathcal{D}_0(p)}{P(p)} \propto \frac{\Sigma(p)}{P(p)}$$

or $(p - p_c)^\rho \propto (p - p_c)^{\mu - \beta}$ implying that $\rho = \mu - \beta$. (5.2-18)

So, *in the case of percolation*, we obtain the following relation between μ and d_s :

$$d_s = \frac{2(d\nu - \beta)}{\mu - \beta + 2\nu} = \frac{2D}{\mu/\nu + D + 2 - d}. \quad (5.2-19)$$

The question has often been raised of whether or not the dynamic exponents are related to the static (geometric) exponents. In 1982, Alexander and Orbach conjectured that for percolation $d_s = 4/3$ independently of d , which

implies, at least for percolation, a relationship between the geometry and dynamics via the equation $d_s = 2D/d_w$ [and hence $d_w = (3/2)D$]. This result is certainly exact for $d \geq d_c = 6$ (the critical dimension for which the mean field is correct), and in numerical studies d_s remains very close to this value $4/3$ (this would lead to a value $d_w = 2.84375$ for $d = 2$ compared with the value 2.87 obtained by numerical simulation). However, the perturbation expansion in $\epsilon = d_c - d$ ($\epsilon \rightarrow 0$) contradicts this supposition as it gives $d_s = 4/3 + c \epsilon + \dots$. In fact, no rigorous proof exists for d , an integer (i.e., $\epsilon = 1, 2, \dots$), and the numerical confirmation is tricky as d_w must have a precision of the order of 10^{-3} .

Table VII: Table of some dynamic exponents for percolation

d	d_w	d_w^ℓ	d_s	μ/n	s/v
2	2.87	2.56	1.31	0.97	0.97
3	3.80	2.80	1.33	2.3	0.85

In the above table we have also shown the values of that exponent, $d_w^\ell = d_w/d_{\min}$, which refers to those walks corresponding to the shortest path or chemical distance ℓ between two points (see Sec. 1.5.1 and Havlin, 1987):

$$\langle \ell(t) \rangle \propto \ell^{1/d_w^\ell}. \quad (5.2-20)$$

Other physical problems, very similar to that of conduction, have been studied in a similar framework. Examples of these are:

- the dielectric constant of an insulator–metal mixture;
- the critical current in a diluted superconductor;
- the flexion modes of a holed plate close to the percolation threshold (see, e.g., Wu et al. 1987); and
- the fracture energy of a composite material.

In Sec. 5.2.3 the dielectric behavior of a composite medium will be examined in greater detail.

Random resistor network: The Coniglio–Stanley model

The critical behavior of the conductivity during the metal–insulator transition of a random resistor network (composed of bonds of resistance R) has been discussed. To find out more about how the current is distributed through the network, especially when the bonds only support a certain maximum current, it is important to have an idea of the connections present in the network. A percolation cluster close to the threshold may be imagined as follows (see also the end of Sec. 3.1.1): the cluster is composed of a *backbone* onto which branches that do not participate in the conduction, because they are dead ends, are grafted (“*white*” bonds). The backbone itself may be partitioned into new subsets: “*red*” bonds, such that cutting any one of them would break

the current in the system (all the intensity is found in these simply connected⁸ bonds); and multiconnected “blue” bonds which constitute what is known as the “blobs” of the infinite cluster (Fig. 5.2.2). Within a region of side L , $1 \ll L \ll \xi$, the number of bonds in each category follows power laws (Coniglio, 1981, 1982; Stanley and Coniglio, 1983, and references therein),

$$\begin{aligned} N_{\text{red}} &\propto L^{D_{\text{red}}}, \\ N_{\text{blue}} &\propto L^{D_B}, \\ N_{\text{white}} &\propto L^D. \end{aligned} \quad (5.2-21)$$

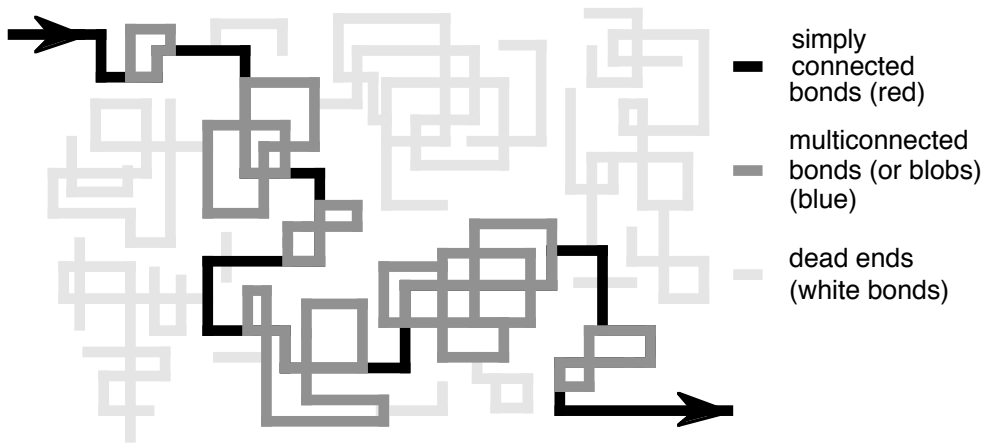


Fig. 5.2.2. Schematic representation of a region of size L ($L < \xi$) of a percolation cluster ($p > p_c$) with current flow (in the direction of the arrows). The finite (not connected) clusters are not shown. A “red bond” is a relative notion which depends on the size of window chosen. These simply connected bonds disappear when $L > \xi$ at the expense of the multiply connected bonds which are uniformly distributed.

The following properties may be observed. The white bonds, through which no current flows, make up the bulk of the cluster, their fractal dimension being D (the same as the infinite cluster). The subset through which the current passes has dimension D_B (see Sec. 3.1.1); the blue bonds are dominant in this and have the same dimension D_B . Finally, the red bonds comprise a very tenuous yet very important subset. They exist (on average) only in domains of size less than or of the order of ξ , the connectivity length. Coniglio (1982) has shown that the red bonds have dimension $D_{\text{red}} = 1/\nu$, where ν is the exponent of the percolation correlation length.

Consequently, if overload is feared in a disordered medium, the further one is from the percolation threshold ($p > p_c$) the weaker is the current in the red

⁸ A bond is simply connected when its removal is sufficient to interrupt the current (this notion depends on L). A part of a cluster is simply connected if the removal of just one bond is sufficient to disconnect it.

bonds of domain size ξ , since the current will then spread throughout these different domains.

The approach just described implies that the random resistor network has a multifractal structure. The multifractal measure to take is the current flowing through each bond.

Multifractal measure in a random resistor network

From what we have just seen, the red (simply connected) bonds carrying all the current correspond in the multifractal distribution to the subset with the maximum intensity $I = I_{\max}$, while the white bonds through which no current flows correspond to the minimum intensity ($I = 0$). Between these two extremes, the multiconnected bonds carry currents of all sizes.

The current distribution in the network (if the maximum current is fixed, $I_{\max} = 1$) is then completely determined by the moments

$$M_q^I \equiv \langle (I/I_{\max})^q \rangle = \langle I^q \rangle = \sum_I n(I) I^q . \quad (5.2-22)$$

The potential distribution for a fixed current is identical (to within a factor R^{-q}) since $V = RI$ in each bond. The resistances of the bonds are taken to be one ($R = 1$). We can also think of this distribution with the total potential fixed ($V_{\max} = 1$),

$$M_q^V \equiv \langle (V/V_{\max})^q \rangle = \langle V^q \rangle = \sum_V n(V) V^q . \quad (5.2-23)$$

The behavior is different in this case because I_{\max} and V_{\max} are related by $I_{\max} = G(L)V_{\max}$, which depends on the size of the sample:

$$M_q^V = G^q M_q^I . \quad (5.2-24)$$

Some moments have a simple interpretation: M_0 is the mean number of bonds in the backbone, M_2^I is the mean resistance (for a fixed total current), and M_2^V is the mean conductance (for a given total voltage). Indeed the mean power dissipated per bond is $R\langle I^2 \rangle = \langle V^2 \rangle/R$, and for simplicity both R and either the total current or voltage are taken as unity. Similarly M_4 can be shown to be related to the amplitude of the noise present in the network.

The coefficient of hydrodynamic dispersion can also be related to the moment of negative order, $q = -1$. Indeed, if we consider a liquid flowing through a porous medium, then the pressure and speed of flow are related by an Ohm's law type of equation. If a colored marker (tracer) is injected through the entry face of the porous medium for a short time, it will disperse in the course of time and the dispersion will be given by the value $\langle t^2 \rangle - \langle t \rangle^2$, where t is the transit time of a colored particle. For each channel (bond) this time is inversely proportional to the current I , and hence $t^q \Leftrightarrow I^{-q}$. Furthermore, the probability of a colored particle being present at the entrance to a channel is proportional to I . Therefore calculating the moment $\langle t^q \rangle$ is equivalent to finding M_{1-q} . Thus, the dispersion of the tracer is related to M_{-1} .

From what we know about the multifractal formalism (Sec. 1.6) the moments M_q obey power laws in the relative size ε of the balls covering the multifractal set. As before (see, e.g., Sec. 1.4.1), it is preferable to vary the size L of the network rather than $\varepsilon = b/L$, b being the length of a bond. Thus,

$$M_q \left(\frac{b}{L} \right) \propto \left(\frac{b}{L} \right)^{-\tau(q)} = \left(\frac{b}{L} \right)^{(q-1)D_q}. \quad (5.2-25)$$

Certain values of τ are thus directly related to known exponents. The exponents, τ^V , at a fixed potential, and, τ^I , at a fixed current are related via the equation

$$\tau^V(q) = \tau^I(q) - q\zeta. \quad (5.2-26)$$

[Eq.(5.2-24) and the scaling behavior of G , Sec. 5.2.1, have been used].

The first values of τ are thus :

$\tau(0) = D_B$: the backbone dimension; $\tau^I(2) = \zeta$: the resistance exponent (Sec. 5.2.1); $\tau^I(\infty) = 1/\nu$: the dimension of the set of red bonds.

The results of numerical simulations giving the distribution of potential and of $\tau^V(q)$ for a given applied voltage are shown in Fig. 5.2.3 (de Arcangélis et al., 1986).

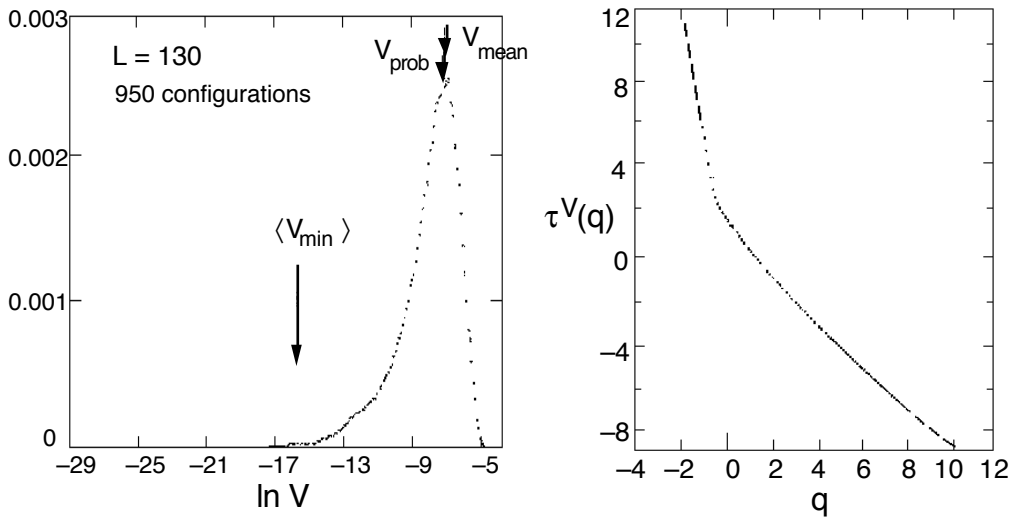


Fig. 5.2.3. Distribution of voltages in a random resistor network at the percolation threshold (figure on the left). The positions of the most probable and mean voltages are indicated. The figure on the right represents $\tau^V(q)$. The high voltage domain roughly obeys a scaling law in L^{-1} , while the low voltage one is in $L^{-6.5}$ (de Arcangélis et al., 1986).

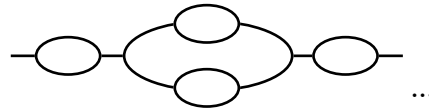
Hierarchical models, conduction in the infinite cluster

Due to the difficulty of carrying out analytic calculations on the infinite percolation cluster and its backbone, various approximate models have been

studied with the aim of understanding the behavior of transport in disordered media. Examples of these are the hierarchical models of Mandelbrot-Given (1984, see Fig. 1.4.6) and of de Arcangelis et al. (1986), in which the generator is



which gives on iteration two:



Besides allowing analytic calculations, these models have the advantage that their structure is fairly similar to that of the infinite cluster backbone. They have “blobs” and red and blue bonds forming subsets whose fractal dimension can be calculated exactly.

Transport in the case of continuous percolation

Continuous percolation, which models a certain number of physical phenomena in where the empty spaces or forbidden regions correspond approximately to randomly distributed spherical zones, exhibits different transport properties (diffusion, electrical conduction, elasticity, permeability) from percolation in a discrete network.⁹

This is due to the special behavior shown by the distribution of the “strength” $g(\delta)$ (conductivity, modulus of elasticity, etc.) of each bond (Fig. 5.2.4), where δ is the thickness of material between two empty regions.

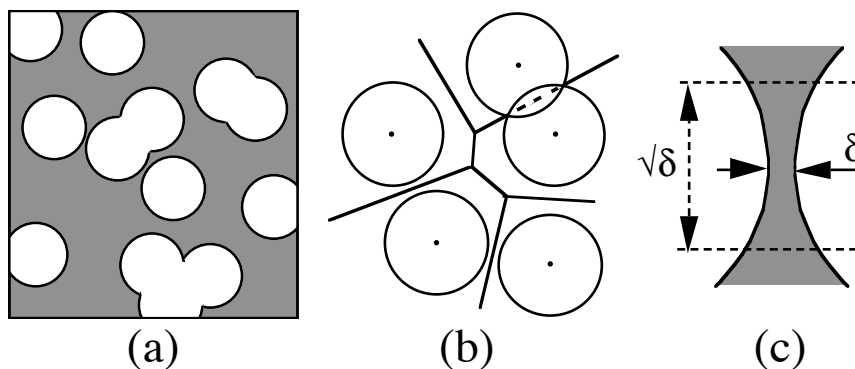


Fig. 5.2.4. Random distribution of empty regions in a material. (a) Model of continuous percolation (here $d = 2$) where the matter is shown in grey. (b) Associated network of bonds. (c) Parameter δ characterizing the “strength” of a bond (its conductivity, modulus of elasticity, etc.)

⁹ Although the geometric critical exponents are the same.

Halperin, Feng, and Seng (1985) demonstrated that by using a uniform random distribution for the empty spheres in a random bond percolation lattice [Fig. 5.2.4(b)], the conductivity distribution g obeys a power law:

$$p(g) \propto g^{-\alpha}.$$

For small values of δ , which are the only ones playing a role in the critical behavior of transport in the neighborhood of the percolation threshold p_c , the “strength” of a bond varies as a function of δ , as $g(\delta) \propto \delta^m$ where m is given by the following table:

“Strength”	$d = 2$	$d = 3$
Diffusion	$m = 1/2$	$m = 3/2$
Constant of flexion force	$m = 5/2$	$m = 7/2$
Permeability		$m = 7/2$

The distribution of g is thus given by $p(g) = h(\delta) (dg/d\delta)^{-1} \propto g^{-\alpha}$ where $\alpha = 1 - 1/m$, since from the distribution of δ , $h(\delta) \rightarrow \text{const.}$, as $\delta \rightarrow 0$.

If we consider the conductance of the system, we find $\alpha = -1$ in $d = 2$, and $\alpha = 1/3$ in $d = 3$. The distribution $p(g)$ is singular in three dimensions. The conductivity is given by Eq. (5.2-8) with μ now depending on α . Straley (1982) has argued for an exponent $\mu(\alpha)$ such that

$$\mu(\alpha) = \min [\mu, \mu_1(\alpha)]$$

with
$$\mu_1(\alpha) = 1 + (d - 2)v + \frac{\alpha}{1 - \alpha}$$

μ is the usual percolation exponent over a lattice (Sec. 5.2.2), and $\mu_1(\alpha)$ is the exponent obtained by taking the conductivity to be limited by the “red bonds” (Fig. 5.2.2) of the associated random network (Halperin et al., 1985). We can therefore see that a crossover exists for a value α_c determined by $\mu = \mu_1$. ($\alpha_c \cong 0.23$ in $d = 2$, $\alpha_c \cong 0.13$ in $d = 3$). This behavior has been numerically verified by Bunde et al. (1986). Benguigui (1986) carried out experiments on conductivity and elasticity in copper sheets, and Lobb and Forrester (1987) have undertaken similar experiments for randomly holed sheets of steel and molybdenum.¹⁰ The exponents obtained are in very good agreement with the theoretical model. Finally, we should add that the diffusion exponents for continuous percolation depend on the manner in which the diffusion takes place; a random walk of fixed step length gives different exponents (Petersen et al., 1989). For further details the work of Bunde and Havlin (1991) may also be consulted.

¹⁰ In order to minimize the plastic deformations (copper and aluminium are more ductile).

5.2.3 Dielectric behavior of a composite medium

The results obtained in the previous paragraph are valid in a more general setting. They may justifiably be continued analytically and frequency dependent effects may be introduced because the scaling law has no singularity.

An example of this occurs when one of the components of a mixture is a *dielectric*. A mixture of a metal of conductivity σ_M and a dielectric of permittivity ϵ_I may be studied by introducing the complex conductivity of the dielectric

$$\sigma_I = \frac{\epsilon_I \omega}{4\pi i} . \quad (5.2-27)$$

If we put $z = \sigma_I/\sigma_M$, the preceding results apply on substituting $\sigma_1/\sigma_2 \rightarrow \sigma_I/\sigma_M$, if $|z| \ll 1$, and $\sigma_1/\sigma_2 \rightarrow \sigma_M/\sigma_I$, if $|z| \gg 1$. In particular, the (complex) conductivity of the medium is given by the expression (Efros and Shklovskii, 1976; Bergmann and Imry, 1977)

$$\Sigma = \text{Re}(\Sigma) + \frac{\epsilon \omega}{4\pi i} , \quad (5.2-28)$$

where, p_M being the concentration of the metal M,

$$\epsilon \propto \begin{cases} \epsilon_I |p_M - p_c|^{-s} & \text{when } |z| \ll 1 \\ (\epsilon_I)^{\frac{\mu}{\mu+s}} \left(\frac{\sigma_M}{\omega}\right)^{\frac{s}{\mu+s}} & \text{when } |z| \gg 1 \end{cases} \quad (5.2-29)$$

$$\text{Re}(\Sigma) \propto \begin{cases} \left. \begin{array}{l} \sigma_M (p_c - p_M)^{-s}, \quad p_M < p_c \\ \frac{\omega^2 \sigma_I^2}{\sigma_M} (p_M - p_c)^{-\mu-2s}, \quad p_M > p_c \end{array} \right\} |z| \ll 1 \\ \left. \begin{array}{l} (\sigma_M)^{\frac{s}{\mu+s}} \left(\frac{\epsilon_I}{\omega}\right)^{\frac{\mu}{\mu+s}} \quad \text{when } |z| \gg 1 \end{array} \right\} |z| \gg 1 \end{cases} \quad (5.2-30)$$

Clearly with this type of approach the general behavior of a network of impedances may be examined. There is an interesting property associated with the loss angle δ , which is related to the phase difference between the real and imaginary parts of the conductivity via the relation $\tan \delta = \text{Re}(\Sigma)/\text{Im}(\Sigma)$. By considering the scaling laws, we can see that at the percolation threshold the loss angle tends to a universal value δ_c as the frequency tends to zero (see the review article by Clerc et al. 1990):

$$\delta_c = (\pi/2) s/(s + \mu) \quad (p = p_c, \omega \rightarrow 0) . \quad (5.2-31)$$

Experiments on powder mixtures (spheres of silvered and unsilvered glass) are in agreement with this behavior.

The relation from which the universal value of the loss angle may be found is simple to deduce from the general form of the conductance suggested by Webman et al. (1975), Efros and Skolovskii (1976), and Straley (1976, 1977). It is the continuation in the complex plane of Eq. (5.2-12) and it may be written¹¹

$$\Sigma(p, \omega) = (R_0)^{-1} |p - p_c|^\mu \Phi_\pm \left(\frac{i\omega}{\omega_0} |p - p_c|^{-(s + \mu)} \right), \quad (5.2-32)$$

where Φ_\pm are the scaling functions above and below the percolation threshold.

5.2.4 Response of viscoelastic systems

Percolation has also been commonly used to describe gelation processes. Some details of this idea, which we was mentioned in Sec. 2.8.1, will be given here, as will its application to the mechanics of gels.

The first studies on gelation leading to a statistical description of the sol-gel transition are due to Flory in 1941 (see Flory, 1971). These involved a mean field approach of the ‘‘Cayley tree’’ variety described in Sec. 3.1.1. In 1976, de Gennes and Stauffer suggested replacing this description with a percolation approach (see de Gennes, 1979, and Stauffer et al., 1982).

An example of chemical gelation by *polycondensation*, concerning the formation of aerogels, was given earlier (in Sec. 5.1.4). In this case polymerization occurs through the elimination of a small molecule (water for silica aerogels). In general terms, bi-, tri-, or quadri- functional monomers create one ($f = 2$), two- or three ($f > 2$)- dimensional lattices. Other processes are equally possible, for example *vulcanization* where bridges form progressively between long chains of polymers, or *additive polymerization* where double or triple bonds are form, allowing the linkage of other clusters.

The earlier dynamic approach can therefore be applied naturally to the mechanical properties of the sol-gel transitions by adopting a percolation model. The rheological properties of a viscoelastic system are in fact characterized by the dynamic viscosity¹² μ and by the complex modulus of elasticity $G = G' + iG''$. The real part $G'(\omega = 0)$ is the modulus of elasticity E of the medium, while its imaginary part G'' representing the dissipation is related to the viscosity by the relation¹³ $G'' = \mu\omega$, a similar relation to the one linking the imaginary part of Σ to the dielectric constant ϵ (Sec. 5.2.3). The general expression for G is written the same way as that for Σ :

¹¹ As the variable in the function Φ_\pm is dimensionless, there is a certain freedom in the way the function is written, which explains why there are several (equivalent !) forms for the conductivity Σ .

¹² The viscosity is sometimes denoted η .

¹³ This relation is comparable with that of the complex conductivity (Sec. 5.2.3) by making the substitution $\epsilon/4\pi \Leftrightarrow \mu$.

$$G(p, \omega) = G_0 \Phi_{\pm} \left(\frac{i\omega}{\Omega_0} \right) \quad (5.2-33)$$

with $G_0 \propto |p - p_c|^\mu$; $\Omega_0 = \omega_0 |p - p_c|^{(s+\mu)}$.

At low frequencies, $\omega \ll \Omega_0$, the beginning of the expansion of Φ may be written

— before formation of the gel, ($p < p_c$),

$$\Phi_{-}(i\omega/\Omega_0) \equiv (i\omega/\Omega_0) B_{-} + (i\omega/\Omega_0)^2 C_{-} + \dots$$

— after the formation of the gel, ($p > p_c$),

$$\Phi_{+}(i\omega/\Omega_0) \equiv A_{+} + (i\omega/\Omega_0) B_{+} + \dots$$

At high frequencies, $\omega \gg \Omega_0$,

$$\Phi_{\pm}(i\omega/\Omega_0) \propto (i\omega/\Omega_0)^\Delta, \text{ where } \Delta = \mu/(s+\mu).$$

These expressions allow the behavior of E and μ at zero frequency to be determined. Finally, as in the previous subsection, the loss angle at threshold tends to a universal value as the frequency tends to zero: $G''/G' \rightarrow \tan(\Delta\pi/2)$. Its dependence on ω is relatively small.

In the case of *chemical gels*, the reaction kinetics are more or less constant and do not display any discontinuity at the gelation threshold. A linear correspondence can be established between the time elapsed from the moment the sol was prepared to its state of gelation (as the kinetics depend on the temperature, the system must be suitably thermalized¹⁴). Thus, between this situation and the percolation model we have the correspondence $t \Leftrightarrow p$. Gelation occurs at time t_g (gelation time) for a concentration, p_c , of chemical bonds. As t_g is approached, the viscosity increases until it diverges according to a law which (in agreement with what we saw earlier) is conjectured to take the form

$$\mu \propto (t_g - t)^{-s} \quad (5.2-34)$$

while the modulus of elasticity E , which was zero up to t_g , becomes positive and obeys a law of the form

$$E \propto (t - t_g)^\mu. \quad (5.2-35)$$

This type of behavior has actually been observed by Gauthier-Manuel et al. (1984). The value they obtained for μ was close to 1.9.

In the case of *physical gels*, the bridging density between the chains is fixed by the temperature or by the concentration of ions causing reticulation. The system is in equilibrium and the relevant parameter is the bond concentration between chains. Fairly precise experiments have been carried out on some very common biopolymers, the pectins (Axelos and Kolb, 1990), in

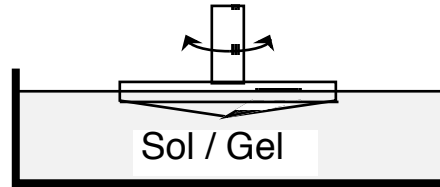
¹⁴ For example an epoxy resin (such as *araldite*) hardens in 24 hours at 20°C, 3 to 4 hours at 40°C, and 45 minutes at 80°C.

which the bond concentration is related to the concentration of Ca^{++} ions causing reticulation. This is again a percolation model.

The torque and phase difference produced by the reaction of the gel (or sol) are measured experimentally by a cone maintained in a forced oscillation of small amplitude. The gel is subject to a shearing $\gamma(t)$, the important parameter being the rate of shearing $\dot{\gamma}$, which has the dimension of frequency. Thus, we may expect the behavior of the viscosity as a function of shearing rate to be of the form

$$\mu(p, \dot{\gamma}) = \mu_0 \Psi_{\pm} \left(\frac{i \dot{\gamma}}{\Gamma_0} \right) \quad (5.2-36)$$

$$\mu_0 \propto |p - p_c|^\mu; \quad \Gamma_0 = \dot{\gamma}_0 |p - p_c|^{(s + \mu)} .$$



Experimental measurements have provided values for pectins, $s \cong 0.82$ and $\mu \cong 1.93$, which agree with a scalar percolation model (i.e., a percolation model together with a model of scalar or entropic vibration). This can be understood in the case of physical gels because here the elasticity of the chains between two bridges is of an entropic nature.

Gels exhibiting tensorial elasticity

Not every gel has exponent values in agreement with percolation models involving scalar elasticity. For instance, we find that for epoxy resins $s \cong 1.4$, for branched polyesters $s > 1.3$ and for gelatine $s = 1.48$, all of which are incompatible with the previous model.

The model may fail for two reasons. First, because the gel's structure cannot be described by a percolation model. For example, hierarchical models have been proposed for aerogels (Maynard, 1989). Second, the elasticity may not be due to entropy. We can see this clearly with aerogels for which the filling fluid is air and where rigidity in bending and compression may be expected. This is just what Vacher et al. (1990) observed (see Sec. 5.1.4 and the phonon–fracton transition). The relation between the spectral dimension d_s and the exponent μ of the modulus of elasticity is unclear, although such a relation does exist in the case of percolation (see Sec. 5.2.2),

$$d_s = \frac{2(d\nu - \beta)}{\mu - \beta + 2\nu} = \frac{2D}{\mu/\nu + D + 2 - d} . \quad (5.2-37)$$

Moreover, spectral dimensions measured in aerosols concern the region of fractal growth (reaction-limited aggregation) between 10 Å and 100–300 Å; whereas viscoelastic properties (s, μ) are measured in the gel in solution. They necessarily relate to distances greater than size of the fractal clusters (1,000 Å to cm).

For the gelation of silica, Gauthier-Manuel et al. (1987) found $\mu \approx 3$, a value which disagrees with scalar percolation but is closer to the model of Kantor and Webman (1984) for which $\mu = 3.6$, to that of Martin (1986) for which $\mu = 2.67$ or even to the classical model for which $\mu = 3$.

Let us finish by mentioning that in the chemical gels we have considered, percolative structures built out of elementary entities (Fig. 3.5.3), in general by reaction-limited growth, constitute the preliminary stage of gelation. These elementary entities should not strictly be considered as rigid and immobile. The description via a percolation model may thus be improved by adding, as Guyon has suggested, effects due to rotations, deformations, and relaxations of the entities which are themselves fractal and immersed in a viscous (*sol*) liquid.

It would, therefore, still be premature to draw definitive conclusions about gels and their elastic properties.

5.3 Exchanges at interfaces

Many natural or industrial processes take place at an interface between two media. These are particularly important in living systems: blood exchanges oxygen and carbon dioxide with the air surrounding us; and tree roots drain water and mineral salts from the soil by selecting they need. Industrial processes also make great use of interface exchanges. In a battery, charging and discharging cause electrochemical reactions to occur at the interfacial between an electrolyte and an electrode. Similarly, heterogeneous catalytic reactions take place at the catalyst's surface (the reaction products then being on the same side of the interface).

When the reaction at the interface involves a large flow of matter, its efficiency will be higher the larger the surface area of the reaction site. Moreover, to reduce congestion, but above all to increase the rapidity of transport, the volume occupied by the interface should be as small as possible. The problem of maximizing the surface/volume ratio leads in a natural way to fractal structures, or more precisely to porous or tree-like structures (as does the need to optimize the flows of the reacting fluids).

The following problem concerning fractal interfaces then arises: knowing the fractal geometry of the interface, what can be said about the transfer properties across this interface?

Electrodes have recently been the object of a number of studies following the experiments of Le Méhauté and Crépy in 1983 (see Sapoval in *Fractals in Disordered Systems*, 1991, for a review of this subject, as well as a discussion

of various experiments by Rammelt and Reinhard, 1990), but remain little understood. While in a linear response régime, the impedance is commonly observed to behave according to a power law with a nontrivial exponent η at low frequencies:

$$Z \propto (i\omega)^{-\eta}. \quad (5.3-1)$$

This is known as *Constant Phase Angle* (CPA) behavior.

Several points concerning transfer across electrodes have been clarified:

— The frequency response of a fractal electrode depends on its electrochemical régime.

— In the diffusion-limited régime the impedance of the electrode depends on its Bouligand–Minkowski dimension (Sec. 1.3.1).

— In the blocking régime the electrode response exhibits constant phase angle (CPA) behavior which in certain special cases has been understood in terms of its geometry. For the moment there is no general description of this phenomenon.

— The microscopic response of a fractal electrode is not proportional to the microscopic transport coefficients, but instead to powers of these parameters. In particular, this can induce errors of interpretation in calculations concerning interface processes.

— Finally, there are exact correspondences between the electrical response of an electrode to a direct current, the diffusive response of a membrane, and the output of a heterogeneous catalyst in a steady state, all having the same geometry.

First of all let us look at the role played by the interfaces in a battery made up of two electrodes separated by an electrolyte.

An electrolytic cell containing a flat electrode of surface area S may be considered as equivalent to a circuit made up of a capacitance $C = \gamma S$, where γ is the specific capacitance of the surface,¹⁴ in parallel with the Faraday resistance R_f . These then act in series with the resistance R_e of the electrolyte. The Faraday resistance is directly proportional to the reciprocal of the rate of electrochemical transfer¹⁵ at the interface and inversely proportional to its surface area ($R_e = r/S$). Two limiting cases may be examined. If there is no electrochemical transfer at the interface, the Faraday resistance is infinite and the electrode is said to be *blocking* or *ideally polarizable*. In the opposite case, it may happen that the *transfer is limited by the diffusion kinetics* of the ions in the electrolyte.

5.3.1 The diffusion-limited regime

¹⁴ This capacitance arises from both the charge accumulation and the surface area. It is obviously defined for a small flat element of unit area.

¹⁵ Like, for instance, in a redox reaction of the type $\text{Fe}^{3+} + e^- \rightarrow \text{Fe}^{2+}$.

In this case, for a flat electrode through which an alternating current of frequency ω flows, the concentration of ions in the neighborhood of the electrode varies locally about a concentration c_0 . The variation is governed by a diffusion law, and it can easily be shown (Sapoval et al., 1988) that the region of oscillating concentration extends over a diffusion layer of width $\Lambda_{\mathcal{D}} \equiv (\mathcal{D}/\omega)^{1/2}$. The number of ions crossing the surface is proportional to the volume $V(\Lambda_{\mathcal{D}})$ occupied by this diffusion layer. It can then be shown that the electrode has a diffusion admittance of the form $\omega c_0 V(\Lambda_{\mathcal{D}})$, where c_0 is a capacitance per unit volume or specific diffusive capacitance. c_0 is a parameter which depends on the ion concentration.

Suppose now that the electrode is rough with associated fractal dimension D (Fig. 5.3.1). The size of $V(\Lambda_{\mathcal{D}})$ is then given exactly by the exterior Bouligand–Minkowski dimension of this fractal surface (Sec. 1.3.3):

$$V(\Lambda_{\mathcal{D}}) = S^{D/2} (\Lambda_{\mathcal{D}})^{3-D}, \quad (5.3-2)$$

so that the admittance of the fractal interface may be written

$$Y_{\mathcal{D}} \propto c_0 S^{D/2} \mathcal{D}^{(3-D)/2} \omega^{(D-1)/2}. \quad (5.3-3)$$

An admittance of this form displays a CPA structure as follows:

$$Y_{\mathcal{D}} \propto (i\omega)^\eta, \quad \text{where } \eta = (D-1)/2. \quad (5.3-4)$$

Thus, in a diffusive regime a fractal electrode exhibits constant phase angle behavior. Of course, the contrary is not true; other sources for this CPA behavior have also been proposed.

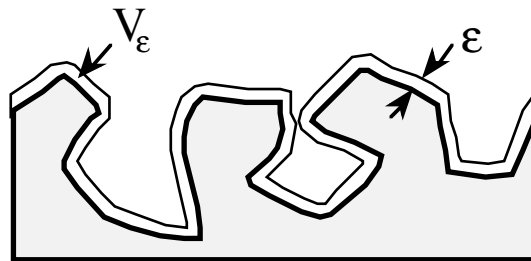


Fig. 5.3.1. External Bouligand–Minkowski dimension associated with an interface. This dimension is defined by $D = \Delta_{ext}(E) = \lim_{\epsilon \rightarrow 0} [d(d - \log V_\epsilon) / \log \epsilon]$, V_ϵ being the volume of a layer of width ϵ covering the external surface.

5.3.2 Response to a blocking electrode

Because blocking electrodes have an infinite Faraday resistance it is impossible for a direct current to flow across them. An electrolytic cell is equivalent to a surface capacitor in series with the resistance of the electrolyte. There are thus two basic parameters in the system, a specific surface capacitance γ and the resistivity ρ of the electrolyte.

From these two parameters we can construct a natural length for the system:

$$\Lambda(\omega) = (\rho\gamma\omega)^{-1} . \quad (5.3-5)$$

This length represents the side of a cube of an electrolyte bounded on one side by the electrode and whose volume at a resistance ρ/Λ is equal to the capacitive impedance of the electrode $1/\omega\gamma\Lambda^2$. If we could assume that Λ was the only length involved in this problem [which is not always the case (Meakin and Sapoval, 1991)], the general form of an admittance Y of a fractal regime exhibiting CPA behavior could be written down. Y would then depend only on L/Λ , L being the dimension of the cell, thus

$$Y = f(L/\Lambda) \propto (i\omega)^\eta \quad \text{or consequently} \quad Y \propto (L/\Lambda)^\eta .$$

Furthermore, a cutoff frequency is reached when $\Lambda > L$. At frequencies lower than this, Y is of the order of L/ρ , so that in the fractal regime we can write

$$Y \propto (L/\rho) (L/\Lambda)^\eta \propto L^{1+\eta} \rho^{\eta-1} (\gamma\omega)^\eta . \quad (5.3-6)$$

Thus, we have the remarkable fact that the response of such an electrode is not a linear function of the surface area of the cell. This relation agrees with exact results obtained from a Sierpinski electrode (Sapoval et al., 1988). It has also been experimentally verified (Chassaing et al., 1990) for ramified electrodes. In different circumstances, Meakin and Sapoval (1991) have shown that for a whole range of *two-dimensional*, self-similar, ramified electrodes the exponent η is related to the fractal dimension by $\eta = 1/D$, an expression already postulated by Le Méhauté and Crépy in 1983. The impedance Y is then proportional to L^{D_1} , where D_1 ($D_1 = 1$ in $d=2$) is the information dimension.

Linear response to d_c excitation

To examine the response of a surface with exchange resistance, r , to direct current excitation, invariance properties mean that we need only replace $\gamma\omega$ by r^{-1} in the expression for the admittance, hence

$$Y_c \propto L^{1+h} r^{h-1} r^{-h} . \quad (5.3-7)$$

Membranes and fractal catalysis

It is interesting to note that the properties mentioned above may be applied in a similar way to a wider class of systems governed by laws of the same type. Examples of these are the diffusion of chemicals across membranes, and heterogeneous catalysis on a fractal catalyst. In certain cases one can predict a

correspondence between the order and the dimension of the reaction (Sapoval, 1991).

5.4 Reaction kinetics in fractal media

The diffusion-limited chemical kinetics of a bimolecular reaction of type



between two chemical species A and B in a homogeneous medium, where the As diffuse while the Bs remain motionless, satisfy an evolution equation

$$-\frac{d[A]}{dt} = k [A] [B], \quad (5.4-2)$$

where k is the reaction constant and $[A]$ is the concentration of A. Smoluchowski showed in 1917 that in three dimensions, k is time independent and proportional to the microscopic diffusion constant, \mathcal{D} , of species A. More precisely, for a lattice model, k is proportional to the efficiency of a random walker on the lattice, that is to say to the derivative with respect to time of the mean number of distinct sites $S(t)$ visited by A and defined in Sec. 5.1.3,

$$k \approx \frac{dS}{dt}. \quad (5.4-3)$$

Strictly speaking this equation is rigorous only for low concentrations of B (i.e., as $[B] \rightarrow 0$), but it turns out to be reasonably accurate for realistic concentrations. These equations have been generalized to the case where both chemicals diffuse, and, in particular, to the case of homo-bimolecular reactions,



whose kinetic equation may be written

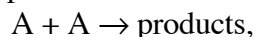
$$-\frac{d[A]}{dt} = k [A]^2. \quad (5.4-5)$$

If A is supplied so as to maintain a steady state, the rate R of reagent production can be written

$$R = k [A]^2, \quad (5.4-6)$$

where the coefficient k is time independent. This situation occurs in dimension $d = 3$ where $S(t) = a t$ (for large enough t , see Sec. 5.1.3).

Heterogeneous kinetics occurring in a fractal structure differ greatly from homogeneous kinetics. Kopelman and his collaborators (Kopelman, 1986) have shown that for the simple reaction



the *diffusion-limited* reaction rate is

$$k = k_0 t^{-h} [A]^2, \quad (t \geq 1), \quad (5.4-7)$$

$$\text{where} \quad h = 1 - d_s/2 \quad \text{if } d_s \leq 2, \quad (5.4-8a)$$

$$h = 0 \quad \text{if } d_s > 2. \quad (5.4-8b)$$

These are expressions easily obtained from Eqs. (5.1-22) and (5.1-23), and the preceding remarks (d_s is the spectral dimension).

When the reaction is supplied with A so as to maintain a steady state, the rate R of reagent production can now be written,

$$R = k_0 [A]^X. \quad (5.4-9)$$

The order X of the reaction is no longer equal to two but to

$$X = 1 + \frac{2}{d_s} = \frac{2-h}{1-h}. \quad (5.4-10)$$

For a percolation cluster structure ($d = 3$), $h \approx 0.33$, and $X \approx 2.5$. For a fractal "dust" with spectral dimension $0 < d_s < 1$ the order of the reaction is greater than 3.

Thus in heterogeneous structures we notice a correlation between energy and geometry, which brings about fractal type kinetics.

The results obtained by taking into account scaling invariance are in good agreement with numerical simulations and with experiment. This type of kinetics applies, for example, to excitations fusion experiments in porous membranes, films, and polymeric glasses.

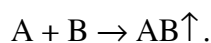
Experiments have been performed on isotopic mixed crystals of naphthalene by Kopelman and his collaborators in the U.S.A., and by Evesque and Duran in France. The mixture of $C_{10}H_{18}$ and $C_{10}D_{18}$ displays a random substitutional disorder and is such that excitations remain localized on the naphthalene clusters at temperatures of 2°K. For triplet excitons:



the effective percolation threshold in the naphthalene clusters is about 8% mole fraction (corresponding to fourth-nearest-neighbor connectivity in a square lattice). In this experiment the phosphorescence (excited triplet \rightarrow fundamental singlet transition), which is proportional to the exciton concentration [A], and the fluorescence (excited singlet \rightarrow fundamental singlet transition), which is proportional to the annihilation rate $d[A]/dt$, are considered separately. The measured slope is $h = 0.35 \pm 0.03$ in agreement with the results from the percolation model:¹⁶ the disorder here is essentially of geometric origin. On the other hand, experiments carried out at 6°K on triplet exciton fusion in naphthalene inside a porous Vycor glass give a larger value of h, $h \approx 0.44$. The structure of Vycor being very different from a percolative structure, but it too involves an energetic disorder superimposed on the geometric one.

¹⁶ In principle the diffusion should be averaged over the infinite cluster (fractal on all scales up to the threshold) and the finite clusters. This provides two contributions of unequal exponent.

Another manifestation of these fractal reaction kinetics is the spontaneous appearance of a segregation (Zeldovich effect) of species A and B in hetero-bimolecular reactions of the type



This phenomenon is also related to the fact that the future evolution depends on the past and particularly on the initial conditions:

(i) Dependence on the past appears in the rate $k = k_0 t^{-h} [A]^2$, which shows that, even with equal concentrations of [A], two samples have different reaction rates if the time elapsed since the start ($t = 1$) of the two reactions is different (it is assumed that initially the distributions are random and $k_0 \equiv k_0^r$ is the same). This effect is, of course, related to the fact that the distribution does not remain random and that a time-dependent segregation occurs.

(ii) Order is present in the steady state itself. For example, consider a photochemical reaction over a disordered structure. If the reacting species A is produced by laser impulsion, its initial distribution may be taken to be random: $k_0 \equiv k_0^r$. If we now produce a steady state by permanently illuminating the sample, we find a partial order there (although the supply of A is randomly distributed), the constant k_0 changes, $k_0 \equiv k_0^{ss}$ (at equal initial concentrations), and a simple empirical criterion for the partial order is then given by the ratio $F = k_0^r / k_0^{ss}$.

These heterogeneous reaction kinetics can also be found to occur in chemistry, biology, geology, and solid state physics, as well as in astrophysics and the atmosphere sciences. For instance, the origin of the separation of charges in both colloids and clouds may be attributed to *reactive segregation*.